Multiple Glass Singularities and Isodynamics in a Core-Softened Model for Glass-Forming Systems

Nicoletta Gnan,[1] Gayatri Das,[2] Matthias Sperl,[3] Francesco Sciortino,[2] and Emanuela Zaccarelli[1,2]
[1]CNR-ISC Uos Sapienza, Piazzale A. Moro 2, I-00185 Roma, Italy
[2]Dipartimento di Fisica, Sapienza Universitá di Roma, Piazzale A. Moro 2, I-00185 Roma, Italy
[3]Institut für Materialphysik im Weltraum, Deutsches Zentrum für Luft-und Raumfahrt, 51170 Köln, Germany
(Received 14 July 2014; revised manuscript received 6 October 2014; published 18 December 2014)

We investigate the slow dynamics of a simple glass former whose interaction potential is the sum of a hard core and a square shoulder repulsion. According to mode coupling theory, the competition between the two repulsive length scales gives rise to a complex dynamic scenario: besides the fluid-glass line, the theory predicts a glass-glass line in the temperature-packing fraction plane with two end points. Interestingly, for critical values of the square-shoulder parameters, such end points can be accessed from the liquid phase. We verify, via extensive numerical simulations, the existence of both points through the observation of an unconventional subdiffusive/logarithmic dynamical behavior. Unexpectedly, we also discover that the simultaneous presence of two end points generates special loci in the state diagram along which the dynamics is identical at all length and time scales.

DOI: 10.1103/PhysRevLett.113.258302 PACS numbers: 82.70.Dd, 64.70.pv, 64.70.Q-, 66.30.J-

Colloidal solutions display a rich variety of dynamical behavior. Experiments have shown that the addition of a short-range attraction to the excluded volume interaction generates multiple dynamically arrested (glassy) states, explored by tuning the interaction strength, the packing fraction, or the range of the attraction [1–6]. These experimental studies agree with predictions based on the mode coupling theory (MCT) [7–11] and numerical simulations [12–17]. Multiple glasses have been revealed in several binary mixtures, including hard [18,19] and soft spheres [20–22]. In star polymers, distinct glasses have been found to surround a region of ergodic state points [23,24]. In all these cases, different microscopic mechanisms compete to generate multiple arrested states and a complex dynamic behavior. Interestingly, logarithmic relaxation has also been reported in solutions of globular proteins [25,26] and in polymeric systems [27,28].

Recently, core-softened potentials with two repulsive length scales have been identified as good candidates for displaying novel glassy dynamics. These models have been introduced to describe disparate systems such as metallic glasses [29], granular materials [30], and penetrable soft particles [31–35], as well as silica [36] and water [37,38]. The square-shoulder (SS) model, i.e., a model whose interaction potential is a hard-core repulsion of extent σ complemented by a repulsive shoulder, belongs to the family of core-softened potentials. For the SS model, MCT calculations have predicted the existence of multiple glass transitions [39]. For specific values of the shoulder width Δ, the temperature T–packing fraction ϕ state diagram is characterized by a nonmonotonic fluid-glass transition line, retracing both upon cooling and upon compression.

Differently from all previously investigated models (both atomic and colloidal), the MCT predicts for the SS system (for small enough Δ) a glass-glass line, completely buried within the glass region and terminating with two end points. Crossing such a glass-glass line, the system discontinuously jumps from one type of glass to another, in a kinetic analogue of a first-order thermodynamic transition [see Fig. 1(a)]. The two end points can be considered as "critical points" beyond which the transition between the two glasses becomes continuous. Borrowing the nomenclature of catastrophe theory [40], the MCT names such end points A_3 singularities. Upon increasing Δ, the glass-glass line progressively moves towards the fluid-glass one and the two lines eventually merge [Figs. 1(b) and 1(c)]. While this happens, each A_3 point moves in the three-dimensional control parameter space (ϕ, T, Δ), until it coalesces with the fluid-glass line. The collision condition defines a set of critical control parameters (ϕ^*, T^*, Δ^*) identifying a higher-order (A_4) singularity. Such a singularity is the only end point accessible from the fluid phase, i.e., in equilibrium conditions. According to the MCT, the SS model is characterized by two distinct A_4 points [Figs. 1(b) and 1(c)]. The dynamics close to singularities (A_3 and A_4) differs from the standard fluid-glass scenario. Instead of the characteristic two-step dynamics, the decay of the density correlators shows a logarithmic dependence on time t. Correspondingly, the mean-squared displacement (MSD) shows a subdiffusive behavior, i.e., $\sim t^a$ with $a < 1$ [11]. Similar features have been observed also in theoretical studies on facilitated models [41], supporting the robustness of the MCT results.

In this Letter we provide numerical evidence of the existence of two A_4 singularities in the SS model, by

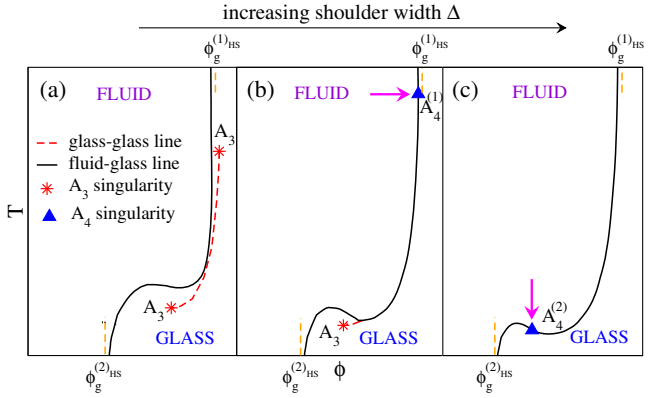

FIG. 1 (color online). Schematic evolution of the MCT dynamic state diagram of the SS system for increasing values of the shoulder width Δ. (a) For small Δ, beside the fluid-glass line (solid line), a disconnected glass-glass line is predicted (dashed line), ending in two A_3 singularities (stars). (b) On increasing Δ, the glass-glass line merges with the fluid-glass line and an A_4 singularity appears when one of the two A_3 points meets the fluid-glass line (filled triangle). (c) At even larger Δ also the second A_3 point eventually intersects the fluid-glass line generating a distinct A_4 singularity (filled triangle). The arrows in (b) and (c) indicate the paths followed to locate the A_4 singularities in the simulations. The vertical dashed lines indicate the glass transitions at high and low densities: while the former happens at the well-known hard sphere glass transition packing fraction $\phi_g^{(1)_{\rm HS}}$, the latter takes place at $\phi_g^{(2)_{\rm HS}} = \phi_g^{(1)_{\rm HS}}/(1+\Delta)^3$.

observing the subdiffusive behavior of the MSD and the logarithmic decay of the density correlators covering several time decades. Additionally, we find a novel dynamic behavior that occurs in the fluid region, generated by the interplay of the two close-by end points. We discover indeed that their simultaneous presence gives rise to special loci in the $T-\phi$ plane along which the self and collective dynamics is identical (isodynamics loci), i.e., where both the short- and the long-time dynamics of the system remarkably coincide at all length scales.

For our investigation we perform event-driven molecular dynamics simulations of a 50:50 noncrystallizing binary mixture of $N = 2000$ particles of species A and B interacting via the pairwise SS potential

$$V_{ij}(r) = \begin{cases} \infty, & r < \sigma_{ij} \\ u_0, & \sigma_{ij} \le r < (1+\Delta)\sigma_{ij} \\ 0, & r \ge (1+\Delta)\sigma_{ij}, \end{cases} \qquad (1)$$

where $i,j = A,B$, σ_{ij} is the hard core between two particles, Δ is the shoulder width, and u_0 is the shoulder height. The size ratio between the two species is $\sigma_{AA}/\sigma_{BB} = 1.2$ and $\sigma_{AB} = (\sigma_{AA}+\sigma_{BB})/2$. The mass of particles is $m = 1$. σ_{BB} and u_0 are chosen as units of length and energy, and the time t is measured in units of $t_0 = \sigma_{BB}\sqrt{m/k_BT}$. T is measured in units of energy ($k_B = 1$). Simulations are performed in the canonical and microcanonical ensemble for a wide range of T and $\phi = (\pi/6)(\rho_A\sigma_{AA}^3 + \rho_B\sigma_{BB}^3)$, where $\rho_A = \rho_B = \rho/2$, $\rho \equiv N/V$ with V the volume of the cubic simulation box.

To locate the A_4 singularities we carry out an extensive study of the dynamics of the SS system. Building on the previous study for $\Delta = 0.15$ [42], where a comparison between simulations and theoretical predictions has provided an estimate of the A_3 points, we restricted our search of the two A_4 points to values of $\Delta \ge 0.17$. Specifically, we have analysed in depth the range $0.17 \le \Delta \le 0.24$, with a mesh of 0.01. For each Δ we have studied the dynamics in a wide window of ϕ and T. Such a lengthy investigation has allowed us to locate the first $A_4^{(1)}$ singularity at the state point ($\phi^{*(1)} \simeq 0.6$, $T^{*(1)} \simeq 0.55$, $\Delta^{*(1)} \simeq 0.21$) and the second $A_4^{(2)}$ at ($\phi^{*(2)} \simeq 0.4$, $T^{*(2)} \simeq 0.15$, $\Delta^{*(2)} \simeq 0.24$). Details of this procedure, based on the mapping of the MCT prediction onto the numerical data, are provided in Ref. [43].

Figure 2 shows the dynamic behavior of the system close to the two A_4 singularities. In the case of $A_4^{(1)}$ (top row panels) we follow the evolution of dynamic quantities on changing ϕ at $\Delta^{*(1)}$ and $T^{*(1)}$ fixed, while for $A_4^{(2)}$ (bottom row panels) we work at fixed $\Delta^{*(2)}$ and $\phi^{*(2)}$ upon changing T, following the paths highlighted in Figs. 1(b) and 1(c). Figure 2(a) shows the increasing subdiffusive behavior of the MSD for the A particles $\langle \delta r_{AA}^2 \rangle$ on increasing ϕ, which extends up to 3 orders of magnitude at $\phi = 0.6$. The B particles behave likewise [inset of Fig. 2(a)]. We stress that even at very high density we do not observe any hint of a plateau in the MSD, a signature of the perfect balance between the two length scales in the interaction potential achieved close to an A_4 singularity. The collective density correlators $\Phi_q^{AA}(t)$ of the A particles display similarly striking features. This is shown in Fig. 2(b), where the correlators are reported for several wave vectors $q\sigma_{AA}$. For a large time window the decay of $\Phi_q^{AA}(t)$ is well described by a second degree polynomial in $\ln(t)$, i.e., $\Phi_q^{AA}(t) \sim f_q - H_q^{(1)}\ln(t/\tau) + H_q^{(2)}\ln(t/\tau)^2$, where f_q, $H_q^{(1)}$, $H_q^{(2)}$ are fit parameters. For a special wave vector $q^{*(1)}$, $H_q^{(2)} \sim 0$ and the correlator displays a pure logarithmic decay. We find $q^{*(1)}\sigma_{AA} = 15.5$. In addition, in the q-vector region explored we observe the convex-to-concave crossover predicted by the MCT [11]. The ϕ dependence of $\Phi_q^{AA}(t)$, reported in Fig. 2(c), shows the growth of the logarithmic regime on approaching $A_4^{(1)}$.

The same analysis has been carried out for $A_4^{(2)}$. As shown in Fig. 1(c), such a singularity lies close to the reentrance, which makes it difficult to explore the region around it by moving along constant T paths. In addition, even along the constant ϕ path (i.e., by varying T) the presence of a reentrant fluid-glass line (imposing its two-step relaxation behavior) partially interferes with the

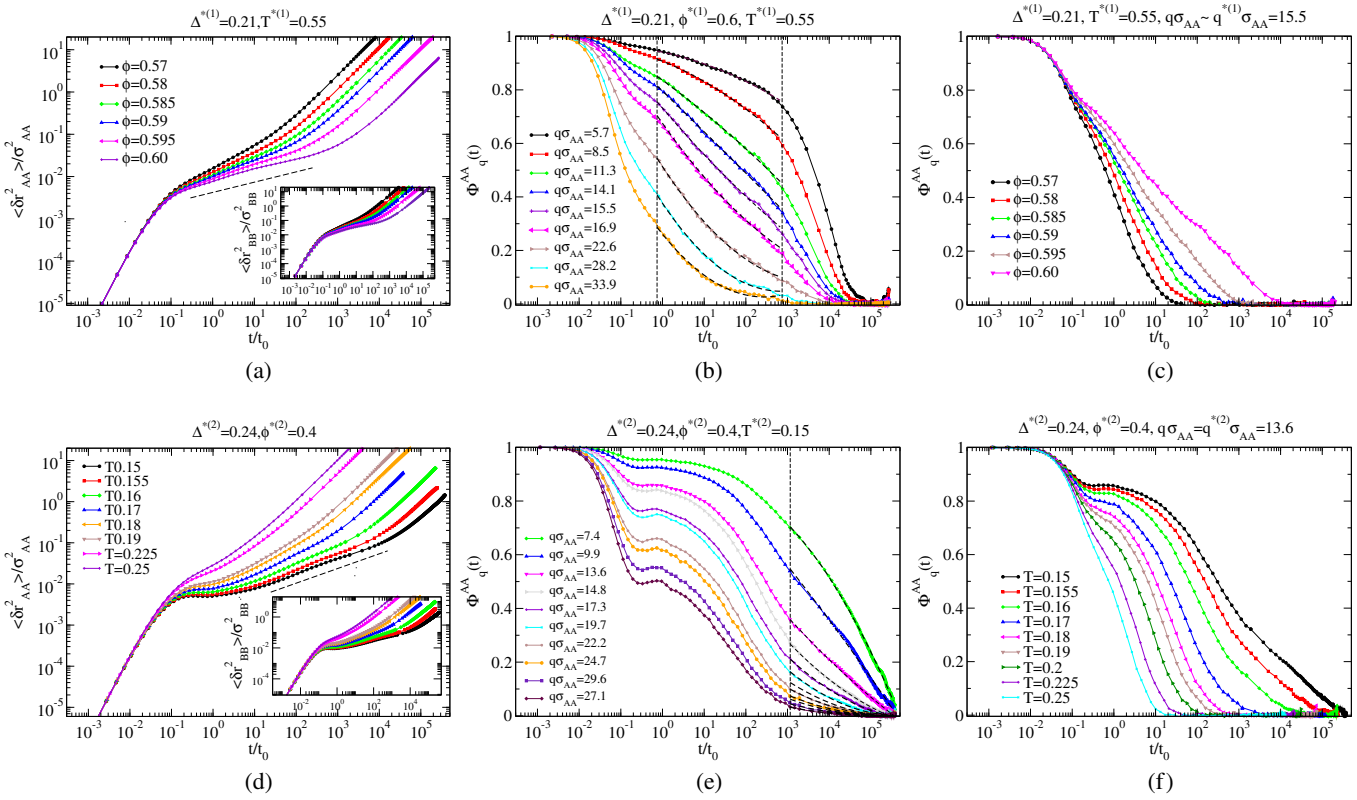

FIG. 2 (color online). Dynamical quantities close to the two singularities $A_4^{(1)} \equiv (\phi^{*(1)} \simeq 0.6, T^{*(1)} \simeq 0.55, \Delta^{*(1)} \simeq 0.21)$ and $A_4^{(2)} \equiv (\phi^{*(2)} \simeq 0.4, T^{*(2)} \simeq 0.15, \Delta^{*(2)} \simeq 0.24)$, along paths shown in Figs. 1(b) and 1(c), respectively. (a) A-particles MSD as a function of the scaled time t_0 for different ϕ at $T^{*(1)}$, $\Delta^{*(1)}$. The dashed line is a power law ($\propto t^{0.3}$) to highlight the subdiffusive regime. The inset shows the MSD for the B species. (b) Collective density correlators of the A species $\Phi_q^{AA}(t)$ evaluated at $A_4^{(1)}$ for different wave vectors $q\sigma_{AA}$. The dotted vertical lines delimit the time window in which $\Phi_q^{AA}(t)$ display a logarithmic behavior. Dashed lines are fits obtained by a second degree polynomial in $\ln(t)$. (c) $\Phi_q^{AA}(t)$ at $T^{*(1)}$, $\Delta^{*(1)}$ as a function of ϕ. (d) MSD for A particles at $\phi^{*(2)}$, $\Delta^{*(2)}$ as function of the scaled time t_0 for different T. The subdiffusive regime is characterized by a power-law $\propto t^{0.37}$. Inset: MSD of B particles. (e) The same as (b) but evaluated at $A_4^{(2)}$. Despite the interference of the fluid-glass line on the dynamics (see text), a long-time logarithmic behavior can be identified. (f) $\Phi_{q^{*(2)}}^{AA}(t)$ at $\phi^{*(2)}$, $\Delta^{*(2)}$ as a function of T.

logarithmic dynamics induced by the A_4 point. As a result, dynamical quantities in Figs. 2(d)–2(f) look different from those obtained for the $A_4^{(1)}$. Figure 2(d) shows $\langle \delta r_{AA}^2 \rangle$ as a function of T for the A and B (inset) particles. In this case the subdiffusive region is preceded by a plateau, a signature of the standard caging effect imposed by the nearby liquid-glass line. The subdiffusive region, the hallmark of the A_4 singularity, is shifted to higher times and extends over almost three decades. The interplay between the fluid-glass line and the A_4 dynamics is also observable in the decay of $\Phi_q^{AA}(t)$ at ($\phi^{*(2)}$, $T^{*(2)}$, $\Delta^{*(2)}$) in Fig. 2(e). For all q vectors the initial part of the structural relaxation displays the typical two-step behavior, but, for longer times, the decay becomes logarithmic. We find a pure logarithmic behavior in $\Phi_q^{AA}(t)$ for $q^{*(2)}\sigma_{AA} = 13.6$. The evolution of $\Phi_q^{AA}(t)$ at $q^{*(2)}\sigma_{AA}$ with T is shown in Fig. 2(f): the long-time decay becomes more and more linear in $\ln(t)$ on approaching $A_4^{(2)}$.

The procedure to locate the A_4 singularities required the investigation of a very large number of state points for several Δ values. During such a process, we have discovered a peculiar dynamic feature of the SS model that we associate with the simultaneous presence of two distinct end points (A_3 or A_4 singularities). Specifically, we find that the competition between these two special points generates loci in the $T - \phi$ plane with invariant dynamics, that we name isodynamics lines. To gain a deeper understanding of such loci we investigate in detail the region in between two A_3 singularities for $\Delta = 0.17$, i.e., for the case schematically shown in Fig. 1(a). We focus on isodiffusivity (iso-D/D_0) [14] paths close to the fluid-glass line ($D_0 \equiv \sigma_{BB}^2/t_0$ accounts for the trivial effect of the thermal velocity), as shown in the inset of Fig. 3(a). Surprisingly, we find that the state points along the iso-D/D_0 curves are characterized not only by the same long-time dynamics but also by the same short- and intermediate-time dependence. Figures 3(a) and 3(b) show, respectively, the MSD and $\Phi_q^{AA}(t)$ as a

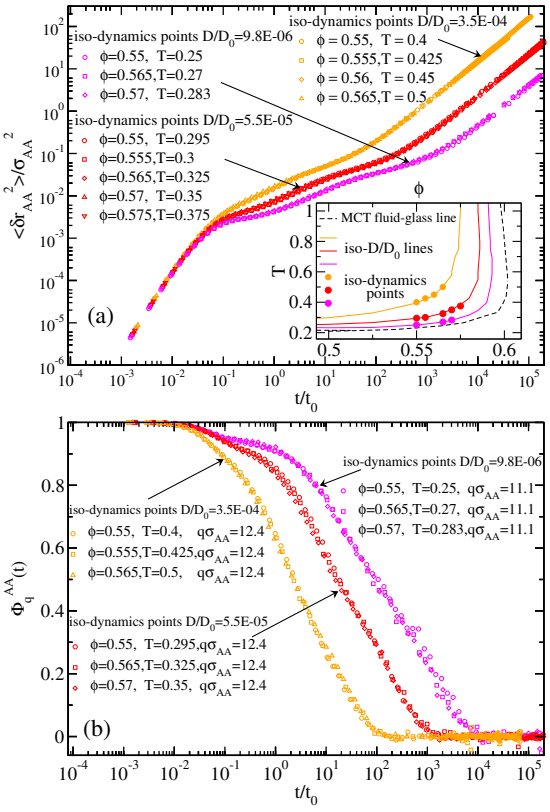

FIG. 3 (color online). Dynamical properties for $\Delta = 0.17$ along three isodynamics lines with rescaled diffusivity $D/D_0 = 3.5 \times 10^{-4}$ (orange symbols), $D/D_0 = 5.5 \times 10^{-5}$ (red symbols), and $D/D_0 = 9.8 \times 10^{-6}$ (magenta symbols). (a) MSD of the A species along the isodynamics lines as a function of t/t_0. (b) Density correlator for the same sets of isodynamics points in (a) as a function of t/t_0. The inset shows the position of the iso-D/D_0 lines and of the expected fluid-glass line [43].

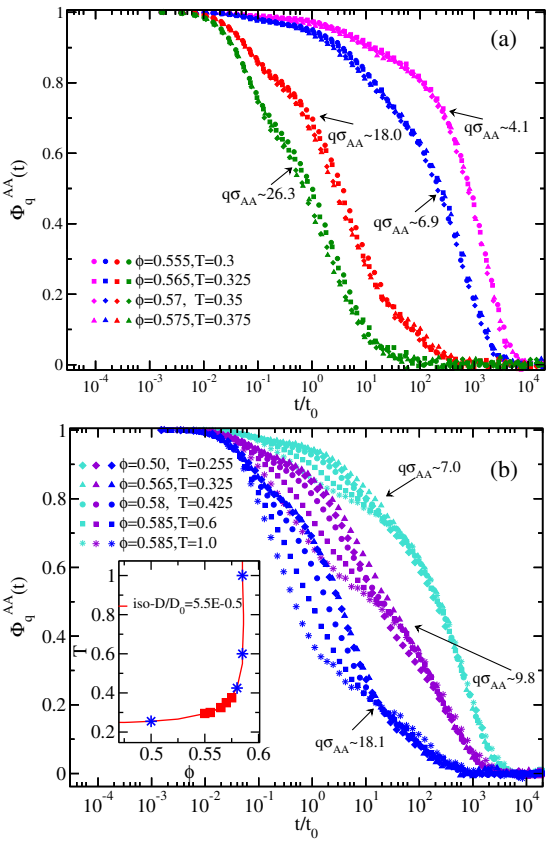

FIG. 4 (color online). $\Phi_q^{AA}(t)$ along the iso-$D/D_0 = 5.5 \times 10^{-5}$ line for $\Delta = 0.17$ at different wave vectors $q\sigma_{AA}$ for (a) isodynamics and (b) nonisodynamics state points. The inset shows the location of such points in the $T - \phi$ diagram. Squares (stars) indicate isodynamics (nonisodynamics) points.

function of t/t_0, along three iso-D/D_0 lines, differing by more than 2 orders of magnitude in D/D_0. For all three iso-D/D_0 sets, the superposition of the curves, at all times and at all length scales, is striking, both in real and in Fourier space. To further support the isodynamics behavior at all length scales we show in Fig. 4(a) the wave-vector dependence of $\Phi_q^{AA}(t)$ for a specific value of D/D_0. Again, superposition of the correlation functions at all times is observed for all q values. These results prove the existence of isodynamics loci, i.e., lines in the $T - \phi$ plane where an identical dynamics is observed. It is interesting to notice that while the dynamics is identical, the structural and thermodynamic properties are not, as discussed in Ref. [43]. Finally we remark that only state points that feel the presence of both singularities obey the invariance. Figure 4(b) shows that the decay of $\Phi_q^{AA}(t)$ does not satisfy the invariance for T and ϕ progressively moving closer to one singularity (but always on the iso-D/D_0 line). In this case, while the long-time dynamics are identical (as one could expect on the basis of the identical diffusion coefficient), the short- and intermediate-time dynamics is now clearly different, indicating that the system explores the nearest-neighbor cages in a different way for each state point. The state points where the isodynamics is or is not observed are indicated in the inset of Fig. 4(b). In Ref. [43] we discuss how the isodynamics behavior is compatible with MCT predictions.

In summary, we have reported numerical evidence of the existence of two A_4 singularities in a simple system with two repulsive length scales. We have confirmed that anomalous dynamical features, such as the logarithmic decay of the density autocorrelation function and the subdiffusive regime in the mean-square displacement, characterize the dynamics close to these points. This result provides (i) one of the most stringent tests of previously formulated MCT predictions, and (ii) evidence that soft colloids could constitute a model system for experimentally testing this highly unconventional behavior. In addition, we unexpectedly discovered that the competition between two singularities gives rise to a nontrivial isodynamics in between the two singularities. Such state points share the same dynamics at all time and length scales. We hope our study will stimulate the experimental search for anomalous dynamics and competing glass transitions in core-softened

systems and in repulsive systems with two competing length scales.

N. G. and E. Z. acknowledge support from Ministero dell'Istruzione, dell'Università e della Ricerca ("Futuro in Ricerca" ANISOFT/RBFR125H0M), G. D., F. S., and E. Z. from EU ITN-234810-COMPLOIDS and M. S. from DFG under FG1394.

[1] F. Mallamace, P. Gambadauro, N. Micali, P. Tartaglia, C. Liao, and S. H. Chen, Phys. Rev. Lett. **84**, 5431 (2000).
[2] T. Eckert and E. Bartsch, Phys. Rev. Lett. **89**, 125701 (2002).
[3] K. N. Pham, A. M. Puertas, J. Bergenholtz, S. U. Egelhaaf, A. Moussaïd, P. N. Pusey, A. B. Schofield, M. E. Cates, M. Fuchs, and W. C. K. Poon, Science **296**, 104 (2002).
[4] S. H. Chen, W.-R. Chen, and F. Mallamace, Science **300**, 619 (2003).
[5] K. N. Pham, S. U. Egelhaaf, P. N. Pusey, and W. C. K. Poon, Phys. Rev. E **69**, 011503 (2004).
[6] X. Lu, S. G. J. Mochrie, S. Narayanan, A. R. Sandy, and M. Sprung, Phys. Rev. Lett. **100**, 045701 (2008).
[7] W. Götze, *Complex Dynamics of Glass-Forming Liquids: A Mode-Coupling Theory* (Oxford University Press, New York, 2009).
[8] L. Fabbian, W. Götze, F. Sciortino, P. Tartaglia, and F. Thiery, Phys. Rev. E **59**, R1347(R) (1999).
[9] J. Bergenholtz and M. Fuchs, Phys. Rev. E **59**, 5706 (1999).
[10] K. Dawson, G. Foffi, M. Fuchs, W. Götze, F. Sciortino, M. Sperl, P. Tartaglia, T. Voigtmann, and E. Zaccarelli, Phys. Rev. E **63**, 011401 (2000).
[11] W. Götze and M. Sperl, Phys. Rev. E **66**, 011405 (2002).
[12] A. M. Puertas, M. Fuchs, and M. E. Cates, Phys. Rev. Lett. **88**, 098301 (2002).
[13] G. Foffi, K. A. Dawson, S. V. Buldyrev, F. Sciortino, E. Zaccarelli, and P. Tartaglia, Phys. Rev. E **65**, 050802 (2002).
[14] E. Zaccarelli, G. Foffi, K. A. Dawson, S. V. Buldyrev, F. Sciortino, and P. Tartaglia, Phys. Rev. E **66**, 041402 (2002).
[15] A. M. Puertas, M. Fuchs, and M. E. Cates, Phys. Rev. E **67**, 031406 (2003).
[16] F. Sciortino, P. Tartaglia, and E. Zaccarelli, Phys. Rev. Lett. **91**, 268301 (2003).
[17] E. Zaccarelli, F. Sciortino, and P. Tartaglia, J. Phys. Condens. Matter **16**, S4849 (2004).
[18] A. Imhof and J. K. G. Dhont, Phys. Rev. Lett. **75**, 1662 (1995).
[19] T. Voigtmann, Europhys. Lett. **96**, 36006 (2011).
[20] A. J. Moreno and J. Colmenero, Phys. Rev. E **74**, 021409 (2006).
[21] A. J. Moreno and J. Colmenero, J. Chem. Phys. **125**, 164507 (2006).
[22] T. Voigtmann and J. Horbach, Phys. Rev. Lett. **103**, 205901 (2009).
[23] C. Mayer, E. Zaccarelli, E. Stiakakis, C. N. Likos, F. Sciortino, A. Munam, M. Gauthier, N. Hadjichristidis, H. Iatrou, P. Tartaglia *et al.*, Nat. Mater. **7**, 780 (2008).
[24] C. Mayer, F. Sciortino, C. N. Likos, P. Tartaglia, H. Loewen, and E. Zaccarelli, Macromolecules **42**, 423 (2009).
[25] M. Lagi, P. Baglioni, and S. H. Chen, Phys. Rev. Lett. **103**, 108102 (2009).
[26] X. Chu, M. Lagi, E. Mamontov, E. Fratini, P. Baglioni, and S. H. Chen, Soft Matter **6**, 2623 (2010).
[27] A. J. Moreno and J. Colmenero, J. Chem. Phys. **124**, 184906 (2006).
[28] A. J. Moreno and J. Colmenero, J. Phys. Condens. Matter **19**, 466112 (2007).
[29] D. A. Young and B. J. Alder, Phys. Rev. Lett. **38**, 1213 (1977).
[30] J. Duran, *Sands and Powders and Grains: An Introduction to the Physics of Granular Materials* (Springer, New York, 1999).
[31] P. Ziherl and R. D. Kamien, Phys. Rev. Lett. **85**, 3528 (2000).
[32] G. Malescio and G. Pellicane, Nat. Mater. **2**, 97 (2003).
[33] N. Osterman, D. Babic, I. Poberaj, J. Dobnikar, and P. Ziherl, Phys. Rev. Lett. **99**, 248301 (2007).
[34] S. V. Buldyrev, G. Malescio, C. A. Angell, N. Giovambattista, S. Prestipino, F. Saija, H. E. Stanley, and L. Xu, J. Phys. Condens. Matter **21**, 504106 (2009).
[35] T. Dotera, T. Oshiro, and P. Ziherl, Nature (London) **506**, 208 (2014).
[36] Y. D. Fomin, E. N. Tsiok, and V. N. Ryzhov, Phys. Rev. E **87**, 042122 (2013).
[37] E. A. Jagla, J. Chem. Phys. **111**, 8980 (1999).
[38] A. de Oliveira, P. A. Netz, and M. C. Barbosa, Eur. Phys. J. B **64**, 481 (2008).
[39] M. Sperl, E. Zaccarelli, F. Sciortino, P. Kumar, and H. E. Stanley, Phys. Rev. Lett. **104**, 145701 (2010).
[40] V. I. Arnold, *Catastrophe Theory*, 3rd ed. (Springer-Verlag, Berlin, 1992).
[41] M. Sellitto, J. Chem. Phys. **138**, 224507 (2013).
[42] G. Das, N. Gnan, F. Sciortino, and E. Zaccarelli, J. Chem. Phys. **138**, 134501 (2013).
[43] See Supplemental Material at http://link.aps.org/supplemental/10.1103/PhysRevLett.113.258302 for additional analysis, which includes Ref. [44].
[44] T. Franosch, M. Fuchs, W. Götze, M. R. Mayr, and A. P. Singh, Phys. Rev. E **55**, 7153 (1997).